# Construction of ozone datasets for the study of climate *

Michael Taylor

Laboratory of Atmospheric Physics, Aristotle University of Thessaloniki (LAP-AUTh), PO Box 149, 54124, Thessaloniki, Greece
mtaylor@auth.gr / URL: http://users.auth.gr/mtaylor/ / ORCID: http://orcid.org/0000-0002-3473-3478 / GS: http://bit.ly/1LAK8io

## ABSTRACT

This short report aims to serve as a summary of the research performed in the last 6 months at LAP-AUTh. Algorithms & models developed and timeseries data products created are described by abstracts describing the main findings. In addition, associated journal articles and conference materials produced for dissemination of the results, are also listed. The report concludes with some thoughts on potential avenues for future work as well as the opportunities for transfer of knowledge to new and existing domains.

**TAGS**: Total Ozone Column, SO2, Brewer Spectrophotometer, NILU-UV Multifilter Radiometer, OMI/Aura, SCIAMACHY/Envisat, GOME/ERS-2, GOME2A/MetepA, CHIMERE, SBUV, Neural Network, Nowcast

* Work done from 02/03/2015-30/09/2016 under contract # 91224 funded by ESA-Phase II/Belgian Institute for Aeronomy (BIRA-IASB)

## 1. RATIONALE

The continuous effort of colleagues at LAP-AUTh over several decades has led to the production of homogeneous records of long and high accuracy time series measurements of total ozone column (TOC) and UV sky irradiances at Thessaloniki with various instruments (e.g. NILU-UV, Brewer). In parallel, as a result of collaboration between LAP-AUTh and other meteorological offices / data providers, a number of multiyear satellite products have also been collected that are co-located with ground truth at Thessaloniki, or which span the national and/or regional domain (e.g. Greece, Europe, the Balkans, the Mediterranean).

Such long time series of co-located ground / satellite data provides a unique opportunity for the development of high precision algorithms to compute new variables such as biological UV products like the Vitamin D estimated dose (VID) and DNA damage estimated dose from ground-based measurements (e.g. NILU-UV irradiances). In addition, models of ground truth variables (e.g. Brewer TOC) from higher frequency (1-minute) measurements (e.g. NILU-UV irradiances) provides a route toward increasing the temporal density of ground truth data such as TOC, photosynthetically-active radiation (PAR) and total global horizontal irradiance (GHI). High frequency (1-minute) estimates of TOC and biological UV products also provide exact satellite coincidence data for cross-validation studies and analyses. Section 2 highlights the algorithms and models developed in this work to achieve these capabilities.

It is worth pointing out that Earth observation (EO) products are now routinely centralized and integrated at data portals held by NASA (http://directreadout.sci.gsfc.nasa.gov/), ESA (https://earth.esa.int/) and GEOSS (http://www.geoportal.org/). Therefore, the new and/or extended datasets produced here can contribute to this collective effort. Real-time products (nowcasts) in particular, offer local stations like Thessaloniki an “early bird” opportunity to have instant access to research results prior to upload and integration of data at the portals. One of the aims of the work described here is to help maximize the impact of LAP-AUTh in the field of climate science by developing new algorithms and data products that can be directly incorporated into EO portals and which will strength LAP-AUTh as a potential partner in future research calls.

## 2. ALGORITHMS & MODELS DEVELOPED

### 2.1 High frequency (1-minute) TOC & exact satellite coincidence cross-validation

A neural network (NN) model was trained to produce high frequency (~1 minute) ground-based estimates of TOC at LAP/AUTh and to then use these to compare with exact overpass satellite TOC data from 4 sensors. In the first stage of model development, ~30,000 records of solar UV spectral irradiance measurements from a NILU-UV multi-filter radiometer coincident with TOC measurements from a co-located Brewer spectroradiometer were used to train a NN to learn the nonlinear functional relation between the radiances and TOC. Close agreement was obtained: $R^2$ = 0.94, RMSE = 8.21 DU, bias = -0.15 DU. A long time series (≥ 1M records) of NILU-UV ground-based measurements were presented as inputs to the NN model to generate high frequency (~1 minute) TOC estimates. In the second stage of development, NILU-NN TOC estimates within ±30 min of overpass time of GOME/ERS-2, SCIAMACHY/Envisat, OMI/Aura and

GOME2/Metop-A TOC data were used to perform a precise cross-validation analysis over Thessaloniki. Close agreement was obtained: $0.88 \leq R^2 \leq 0.90$ for all sky conditions and $0.95 \leq R2 \leq 0.96$ for clear sky conditions. The mean fractional differences are found to be -0.67% ± 2.15%, -1.44% ± 2.25%, -2.09% ± 2.06% and -0.85% ± 2.19% for GOME, SCIAMACHY, OMI and GOME2 respectively for the clear sky cases. The nearly constant standard deviation (~ ±2.2%) across all sensors testifies directly to the stability of both the GODFIT_v3 algorithm and also the NN model for providing coherent and robust TOC records. Biases were found to be <5 DU and suggest that systematic errors are low.

**MAIN FINDINGS**:

1) a NN model combined with high frequency NILU-UV irradiances provides the capability for the generation of high frequency (1-minute) ground-based TOC estimates
2) the NN estimated TOC values agree well with satellite retrievals at overpass with fractional differences of less than 3%
3) the GODFIT_v3 algorithm is stable for OMI,GOME,GOME2 and SCIAMACHY

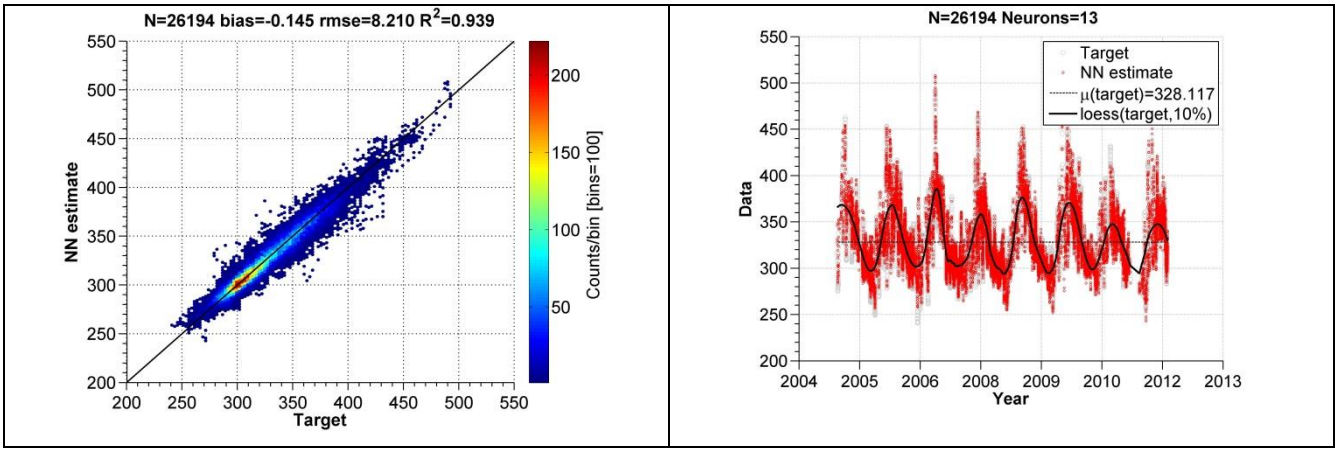

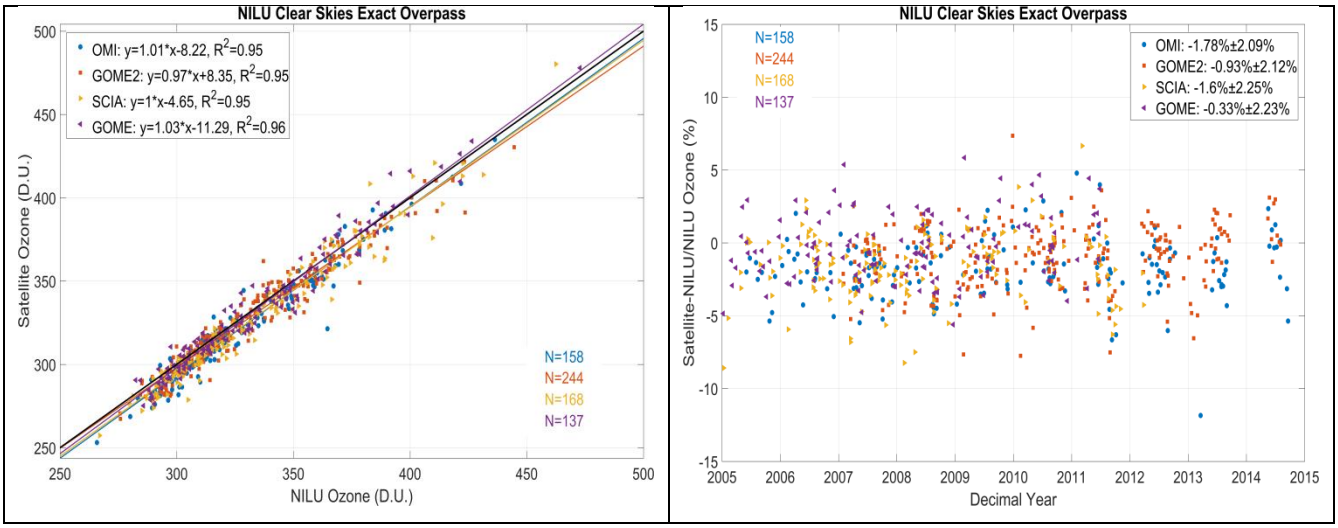


***Figure 1*** *NN training and satellite validation. (Top Left) Cloud density plot of the regression of the NN estimates on the coincident Brewer derived TOC. (Top Right) Time series of the NN estimates and coincident Brewer derived TOC. Also shown is the mean measured value as well as a LOWESS fit to the Brewer derived TOC data to indicate the annual variation. (Lower Left) Scatter plot of the satellite TOC versus NILU-NN TOC for each of 4 satellite sensors 1-minute within exact overpass time. (Lower Right) Percentage differences between satellite TOC and NILU-NN TOC for 4 satellite sensors as a time series at the exact overpass.*

Articles and conference materials published or submitted:

- Zempila, M.M., Taylor, M., Koukouli, M.E., Lerot, C., Fragkos, K., Fountoulakis, I., Bais, A., Balis, D.S., van Roozendael, M. (2016) *NILU-UV multi-filter radiometer total ozone columns: comparison with satellite observations over Thessaloniki, Greece*. **Atmospheric Environment**. [submitted]
- Zempila, M.M., Taylor, M., Koukouli, M.E., Lerot, C., Bais, A., Fragkos, K., Fountoulakis, I., Balis, D.S., van Roozendael, M., Kazadzis, S. (2016) *Evaluation of satellite total ozone observations with a ground based NILU-UV radiometer: in preparation for TROPOMI/S5P*. **European Space Agency Atmospheric Composition Validation and Evolution (ESA/ACVE) 2016, 18-20 October, Frascati (Rome), Italy**. http://congrexprojects.com/2016-events/16c16-acve. [abstract submiited]
- Zempila, M.M., Taylor, M., Koukouli, M.E., Bais, A., Lerot, C., Fragkos, K., Fountoulakis, I., Drosoglou, T., Gketsi, F., Kazadzis, S., Balis, D.S., van Roozendael, M. (2016) *High frequency retrieval of total ozone from a ground-based NILU-UV radiometer using a neural network model: validation of the model and evaluation of satellite observations*. **Quadrennial Ozone Symposium (QOS) 2016, 4–9 September 2016 Edinburgh**. http://www.ozone-symposium-2016.org. [abstract submiited]
- Koukouli, M.E., Lerot, C., Fragkos, K., Fountoulakis, I., Zempila, M.M., Taylor, M., Balis, D.S., Bais, A., van Roozendael, M. (2016) *Validation of the long term ESA Ozone-CCI GODFIT_v3 Total Ozone Record using three different ground-based instruments at a Northern mid-latitude station*. **Quadrennial Ozone Symposium (QOS) 2016, 4–9 September 2016 Edinburgh**. http://www.ozone-symposium-2016.org. [Poster]

## 2.2 High frequency (1-minute) biological UV products & exact satellite coincidence cross-validation

In an analogous approach to (2.1), but requiring a synergy of ground-based data models to provide all training data, a single NN model was then used to produce high frequency (~1 minute) ground-based estimates of 3 photobiological UV effective dose products: the erythemal UV (CIE), vitamin D and that for DNA damage. These were then used to compare with exact overpass satellite TOC data from 4 sensors. Ground-based data from a Brewer MkIII spectroradiometer, a NILU-UV multifilter radiometer, as well as a co-located YES UVB-1 pyranometer deployed for the period 2005-2015 were used. To produce ground-based estimates of the biological UV products, the SCHICrivm algorithm was applied to Brewer data and weighted with the action spectra for erythemal UV, the formation of vitamin D in the human skin and the DNA damage, and used to derive empirical relations for the retrieval of these products from the YES data. A NN was

then trained to learn the nonlinear functional relation between NILU-UV irradiances and the Brewer-based photobiological effective dose products. The long coincident time series (≥ 1M records) of NILU-UV ground-based photobiological effective dose products generated from the NN were then used for ground-based comparisons with those obtained by the Brewer and the YES instruments. NILU-UV NN retrievals and YES retrieved dose rates did not differ by more than 0.07% for the erthemal UV, 1.3% for vitamin D and 5% for DNA damage, with some improvement being noticeable for clear sky cases. Satellite retrievals are then used to provide an important comparison for the ground-based estimates obtained by the NILU-UV NN. OMI/Aura surface UV irradiance data from 2004 to 2014 which includes the erythemally-weighted daily dose and erythemal dose rate both at the overpass time and also at local solar noon were used as well as those provided by the SCIAMACHY/Envisat and GOME2/Metop-A Joint UV Product. Comparison of the erythemal UV dose rate at exact OMI overpass time showed excellent agreement within 14% for all sky and clear sky cases. At local noon R2 is in the range 0.88-0.93 depending on sky conditions and is in the range 0.90-0.98 for daily-integrated values. The SCIMACHY/GOME2 daily erythemal UV product was ~ 15% higher than the ground-based estimate but, despite the presence of a visually apparent seasonal pattern, the R2 value was again found to be robustly high and equal to 0.92. Both SCIAMACHY/GOME2 daily vitamin D and DNA damage doses were found to be ~ 50% higher than surface estimates.

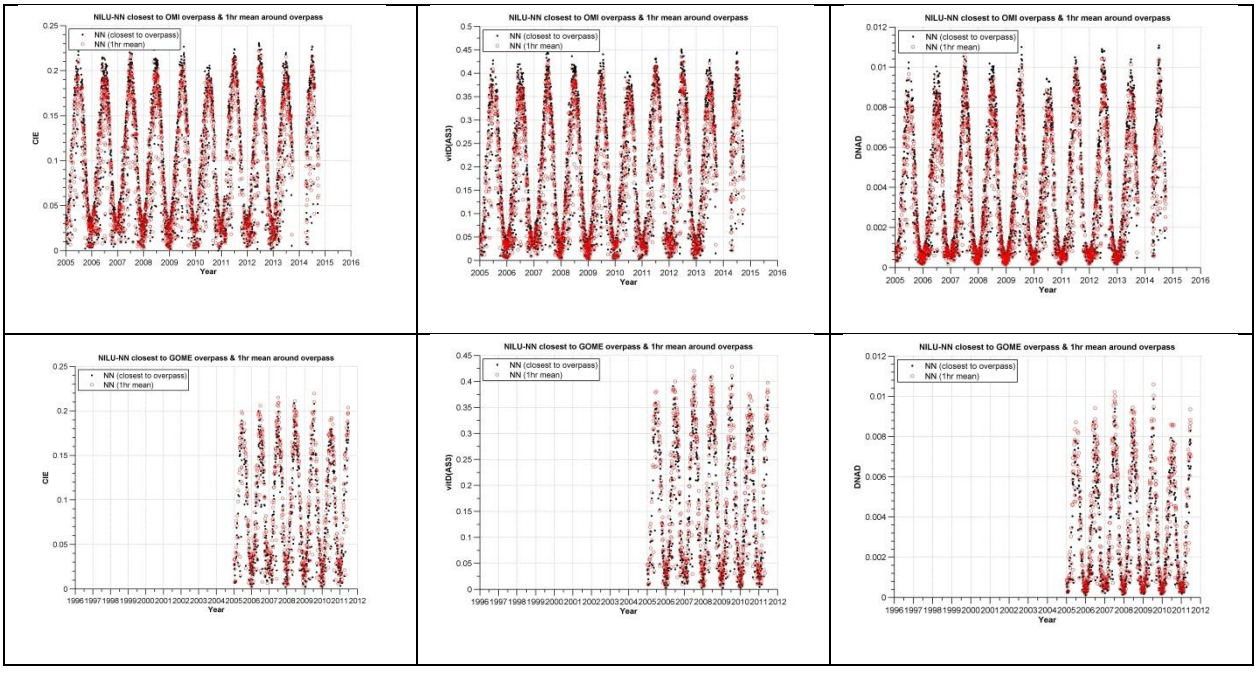

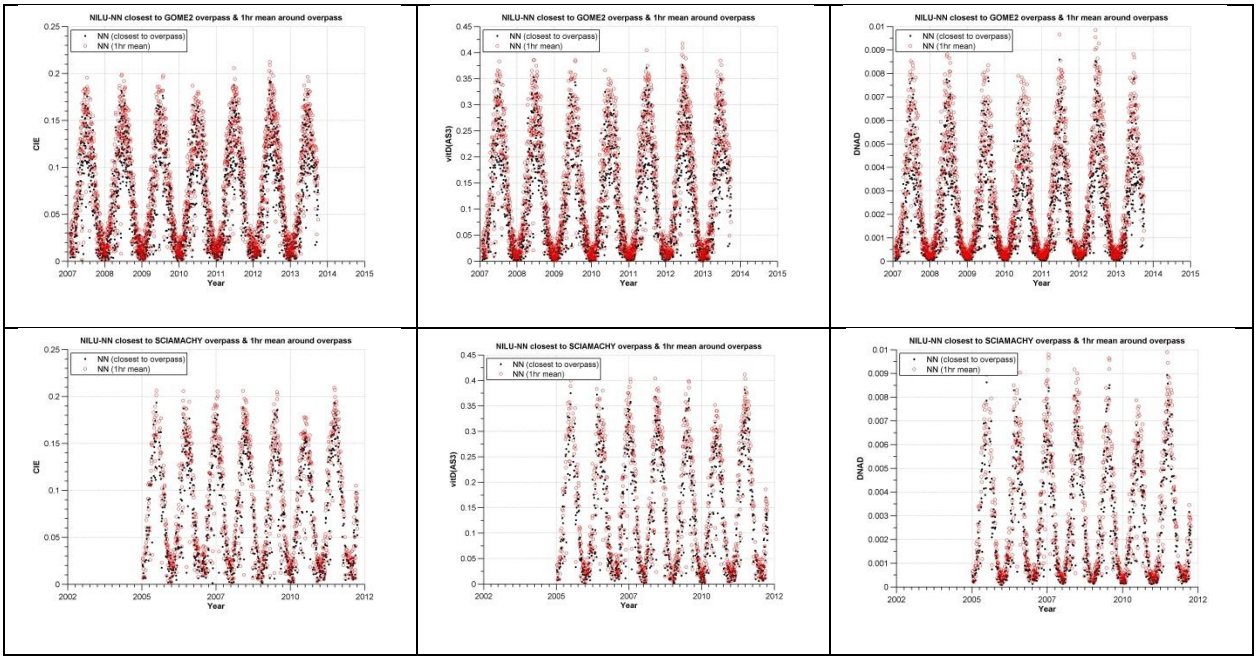


***Figure 2.*** *The NILU-NN simulated time series of CIE (left panels), vitamin D (center panels) and DNA damage dose rates (right panels) closest to overpass time and the estimated overpass value from the mean of values within 1hr of overpass for OMI (top row), GOME (2nd row), GOME2 (3rd row) and SCIAMACHY (bottom row).*

**MAIN FINDINGS**:

1) the SCHICrivm algorithm in conjunction with a synergy of instruments allowed creation of a decade of ground truth estimates of biological UV products (CIE, VID and DNA)
2) a NN can be trained on NILU-UV multi-filter radiometer irradiances at 5 different wavelengths together with weighted action-spectra from a Brewer MKIII spectrophotometer to produce 1-minute time series of erythemal CIE, vitamin D and DNA damage dose rates
3) NN estimated erythemal UV dose rates can be directly compared with YES calibrated measurements and appropriate methodologies can be applied to the original YES data to also produce vitamin D and DNA damage dose rates at the same temporal resolution as the NILU-UV instrument (1-minute)

Articles and conference materials published or submitted:


- Zempila, M.M., Taylor, M., Fountoulakis, I., Koukouli, M.E., Bais, A., Arola, A., van Geffen, J., van Weele, M., van der A, R., Kouremeti, N., Kazadzis, S., Meleti, C., Balis, D.S. (2016) *Photobiological effective dose products from NILU-UV multifilter radiometer irradiances using a neural network: validation and evaluation with ground measurements and satellite estimates over Thessaloniki, Greece*. **Atmospheric Environment.** [submitted].
- Zempila, M.M., Taylor, M., Koukouli, M.E., Fountoulakis, I., Bais, A., Arola, A., van Geffen, J., van Weele, M., van der A, R., Meleti, C., Balis, D.S., Kouremeti, N., Kazadzis, S. (2016) *Evaluation of Satellite Photobiological Effective Dose Products with a ground-based NILU-UV*

*Radiometer: in preparation for TROPOMI/S5P*. **European Space Agency Atmospheric Composition Validation and Evolution (ESA/ACVE) 2016, 18-20 October, Frascati (Rome), Italy**. http://congrexprojects.com/2016-events/16c16-acve. [abstract submiited]

- Zempila, M.M., Taylor, M., Fountoulakis, I., Koukouli, M.E., Bais, A.F., Arola, A., van Geffen, J., van Weele, M., van der A, R., Kouremeti, N., Kazadzis, S., Meleti, C., Balis, D.S. (2016) *CIE, Vitamin D and DNA damage: a synergistic study in Thessaloniki, Greece*. Proceedings of the **European Space Agency Living Planet Symposium (ESA/LPS) 2016, 9-13 May, Prague, Czech Republic**.http://lps16.esa.int. [Conference Paper + Poster]

### 2.3 Generic PAR to GHI (and vice-versa) model

Report on the construction of generic models to calculate photosynthetically active radiation (PAR) from global horizontal irradiance (GHI), and vice versa. The study took place at stations of the Greek UV network (UVNET) and the Hellenic solar energy network (HNSE) with measurements from NILU-UV multi-filter radiometers and CM pyranometers, chosen due to their long (≈1 M record/site) high temporal resolution (≈1 min) record that captures a broad range of atmospheric environments and cloudiness conditions. The uncertainty of the PAR measurements is quantified to be ±6.5% while the uncertainty involved in GHI measurements is up to ≈±7% according to the manufacturer. It was shown how multi-linear regression and nonlinear neural network (NN) models, trained at a calibration site (Thessaloniki) can be made generic provided that the input–output time series are processed with multi-channel singular spectrum analysis (M-SSA). Without M-SSA, both linear and nonlinear models perform well only locally. M-SSA with 50 time-lags is found to be sufficient for identification of trend, periodic and noise components in aerosol, cloud parameters and irradiance, and to construct regularized noise models of PAR from GHI irradiances. Reconstructed PAR and GHI time series capture ≈95% of the variance of the cross-validated target measurements and have median absolute percentage errors <2%. The intra-site median absolute error of M-SSA processed models were ≈8.2±1.7 W/m2 for PAR and ≈9.2±4.2 W/m2 for GHI. When applying the models trained at Thessaloniki to other stations, the average absolute mean bias between the model estimates and measured values was found to be ≈1.2 W/m2 for PAR and ≈0.8 W/m2 for GHI. For the models, percentage errors are well within the uncertainty of the measurements at all sites. Generic NN models were found to perform marginally better than their linear counterparts.

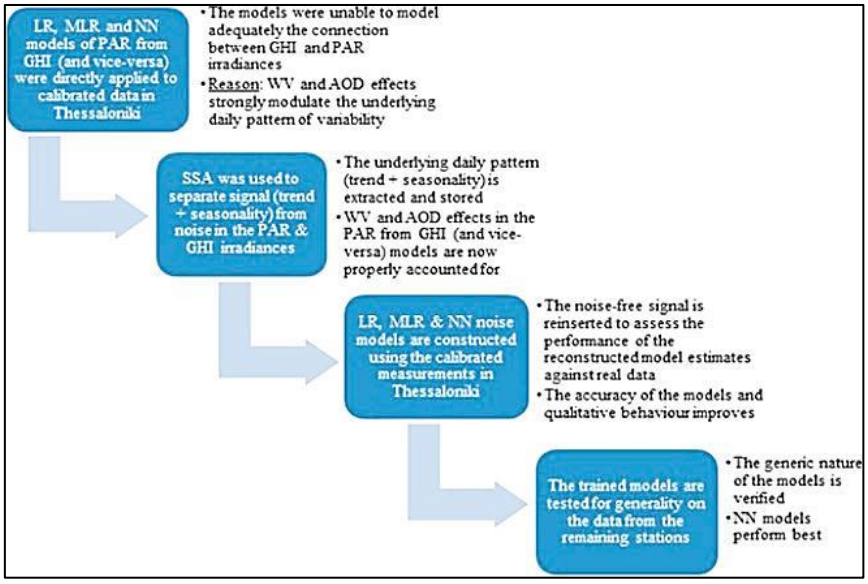


***Figure 3.*** *A schematic of the rationale for the model configuration and their implementation.*

**MAIN FINDINGS**:

1) Generic linear regression and nonlinear neural network models of PAR and GHI are constructed.
2) The LibRadtran UVspec model is used to calibrate PAR data and convert counts to irradiance.
3) Multi-channel singular spectrum analysis is central to regularization of PAR and GHI time series.
4) PAR and GHI models use solar zenith angle, aerosol optical depth and water vapor as inputs.
5) Nonlinear neural network models are found to perform slightly better than linear models.

Published article:

- Zempila, M.M., Taylor, M., Bais, A., Kazadzis, S. (2016) *Modeling the relationship between photosynthetically active radiation and global horizontal irradiance using singular spectrum analysis*. **Journal of Quantitative Spectroscopy and Radiative Transfer** 182:240–263. www.dx.doi.org/10.1016/j.jqsrt.2016.06.003.

### 2.4 High sensitivity & high frequency (1-minute) cloud screening algorithm

A new method for detecting the presence of clouds by their impact on daily UV and PAR irradiance measurements was developed. In Thessaloniki, a NILU-UV multi-filter actinometer has been in regular operation since 2005 and provides continuous, calibrated and high temporal resolution (≈1 min) measurements of UV irradiance in 5 wavelength bands, and also photosynthetically active radiation (PAR) via a sixth channel in the visible part of the spectrum. In this study, singular spectrum analysis (SSA) was applied on a daily basis to the complete annual record of daily UV and PAR measurements (≈800/day) for 2014. Threshold conditions and selection criteria based on the curvature of trend, periodic and noise components extracted by SSA are then used to identify periods where the expected clear sky irradiance is attenuated due to the presence of clouds. Separate cloud detection algorithms were developed for UV and PAR due to

differences in their spectral attenuation. The algorithms are tested for consistency with reference to observations of cloud in co-located RGB images recorded every 15 minutes by an all sky camera in the Laboratory of Atmospheric Physics (LAP/AUTh) throughout 2014.

**Fig. 4** presents 9 all sky images for the "Broken Cloud" day 24/09/2014 which had a highly variable irradiance curve in the morning. In accordance with the results of the cloud detection algorithm, images outlined in red are clear sky and those outlined in blue are cloud scenes. Note how, attempting to making such distinctions by eye would lead to error.

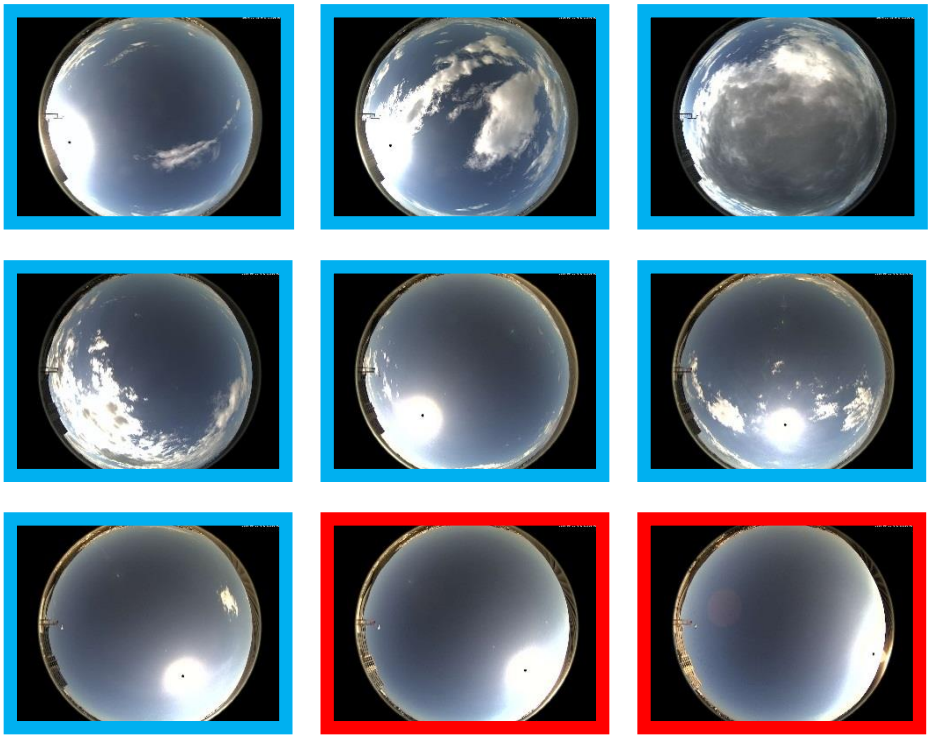

***Figure 4.*** *All sky camera images on the24th of September, 2014 coincident with 1-minute NILU-UV irradiance measurements sampled every 15 minutes for cloud cases (blue) and clear cases (red) highlighted in accordance with the results of the cloud detection algorithm applied to PAR measurements.*

Conference material:

- Zempila, M.M., Taylor, M., Fountoulakis, I., Bais, A., Kazadzis, S., Fragkos, K. (2016) *Introducing a cloud screening detector using global horizontal irradiances in UV and PAR in Thessaloniki, Greece*. In: Perspectives on Atmospheric Sciences, Springer Atmospheric Sciences, ISBN: 978-3-319-35094-3, Proceedings of the **13th International Conference on Meteorology, Climatology and Atmospheric Physics (COMECAP) 2016, 16-19 September, Thessaloniki, Greece**. http://comecap2016.geo.auth.gr. [Paper + Talk]

## 2.5 Nonlinear trend & seasonality detection algorithm

We report on the development of a fast and robust algorithm to detect and statistically-test for the existence of stable cycles in quasi-periodic oscillations present in noisy atmospheric time series that contain short data gaps. This 'seasonality detector' combines singular spectrum analysis (SSA) of interpolated data in the time domain with hypothesis testing associated with spectral estimates in the

frequency domain. While SSA provides an initial time-series decomposition into a slowly varying nonlinear trend, total noise and quasi-periodicity, it is unable to identify the frequency of individual cycles, if present. We show how cycle detection can be achieved in the frequency domain by applying a chi-squared test to the smoothed periodogram computed with the discrete Fourier transform and Daniell filters such that: i) spectral estimates at peak frequencies account for the largest proportion of the total variance and ii) the lower confidence bound on the spectral estimates is distinct from an equivalent area noise continuum used to construct the null hypothesis at the 95% level. As a part of the model development, we introduce a gap-filling algorithm and assess the impact of porosity on the statistical properties of surrogate time series of interpolated monthly mean anthropogenic SO2 loads extracted from ten years of OMI/Aura satellite observations between 2005 and 2015 using the BIRA/IASB algorithm. We demonstrate that a robust and objective implementation of SSA is capable of guaranteeing strict stationarity of the detrended time series and we correlate the extracted trend against other linear and nonlinear regression methods. Statistically-significant frequencies identified in the quasi-periodic component of the surrogate data are cross-validated against those of the wavelet power spectrum, and we end with a comparison of the nonlinear SSA time series model of the time series against their Fourier reconstruction using a linear trend and statistically-significant cycles. We provide a MATLAB implementation of the seasonality detector to facilitate its uptake and further development. Paper II applies this methodology to a high volume sample of 454 time series of satellite measured SO2 over major cities and power stations in China.

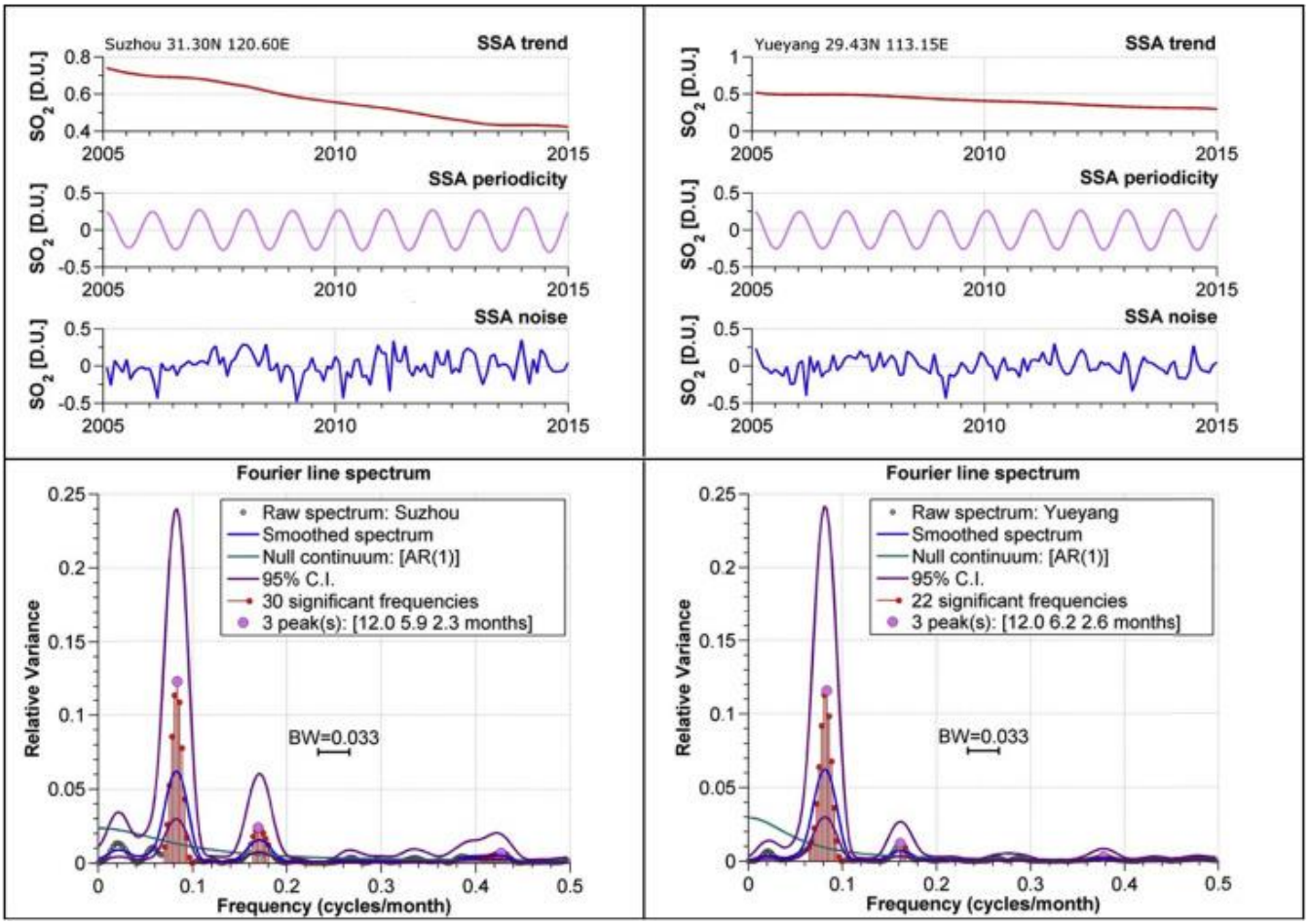


***Figure 5.*** *[Upper panels] The total extracted trend, periodicity and noise SSA components for Suzhou (left) and Yueyang (right). [Lower panels] The detection of annual and bi-annual cycles (12 and 6 months respectively) using the method of Taylor et al. (2016a) for the SSA detrended time series at Suzhou (left) and Yueyang (right). The raw spectrum is given by the grey circles, the smoothed spectrum by the blue line, the null continuum by the green line, the 95% confidence interval (C.I.) by the purple line, the significant DFT frequencies by red circles and the actual peaks by pink filled circles.*

Scientific articles published and in preparation, plus conference material:

- Koukouli, M.E., Balis, D.S., van der A, R., Theys, N., Hedelt, P., Richter, A., Krotkov, N., Li, C., Taylor, M. (2016) *Anthropogenic sulphur dioxide load over China as observed from different satellite sensors*. **Atmospheric Environment**, Online: 6 September, 2016. http://dx.doi.org/10.1016/j.atmosenv.2016.09.007.
- Taylor, M., Koukouli, M.E., Theys, N., Bai, J., Zempila, M.M., Balis, D.S., van Roozendael, M., van der A, R. (2016) *A robust seasonality detector for geophysical time series: application to satellite SO2 observations over China*. In: Perspectives on Atmospheric Sciences, Springer Atmospheric Sciences, ISBN: 978-3-319-35094-3, Proceedings of the **13th International Conference on Meteorology, Climatology and Atmospheric Physics (COMECAP) 2016, 16-19 September, Thessaloniki, Greece**. http://comecap2016.geo.auth.gr. [Paper + Oral]
- Taylor, M., Koukouli, M.E., Theys, N., Bai, J., Zempila, M.M., Balis, D.S., van Roozendael, M., van der A, R., Meko, D., Ghil, M. (2016) *A robust seasonality detector for time series affected by periodic drivers and sporadic events: I. method based on SSA and the smoothed periodogram*. **Nonlinear Processes in Geophysics.** [draft stage]
- Taylor, M., Koukouli, M.E., Theys, N., Bai, J., Zempila, M.M., Balis, D.S., van Roozendael, M., van der A, R., (2016) *A robust seasonality detector for time series affected by periodic drivers and sporadic events: II. application to satellite SO2 estimates*. **Nonlinear Processes in Geophysics.** [in preparation]

## 2.6 Long-term trend analysis of TOC

With 33 years of continuous measurements, Thessaloniki has one of the world's longest time series of the total ozone column (TOC) derived from a Brewer 005 spectrophotometer that was first deployed in March 1982. The multi-decadal time series provides a unique dataset for analyzing long-term changes in TOC and its parametric dependencies. Here we apply two multivariate time series methodologies: i) multi-channel singular spectrum analysis (M-SSA); which separates the TOC time series into statistically-significant trend, periodic and noise components, and ii) a multiple linear regression (MLR) model; that accounts for the effect of known periodic and non-periodic signals (solar cycle, QBO, NAO and ENSO) on long-term linear monthly trends in TOC at mid-latitudes. We confirm that the negative trend in TOC exhibits a turning point during 1997 coinciding with a peak in the amount of the ozone-depleting substances. Post-1997 ozone recovery, while not statistically-significant, is shown to be evident for the majority of the months that follow, especially during winter. We use the insight provided by M-SSA and the coefficients in the MLR model to assess whether post-turnaround trends are influenced by other factors of dynamical origin such as changes in the Brewer-Dobson circulation.

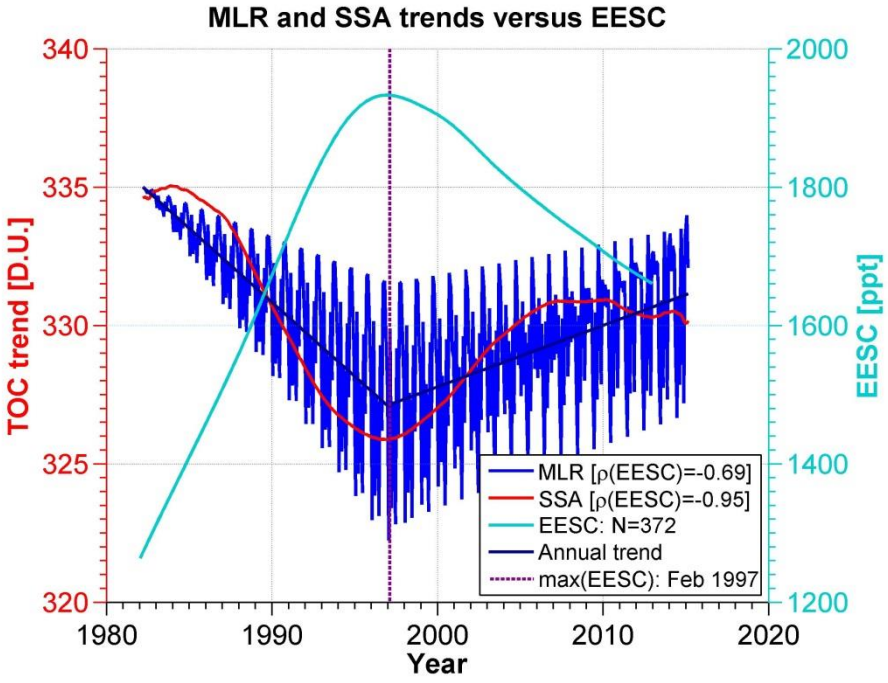


***Figure 6.*** *Left axis: Monthly mean values of the TOC trend as calculated by the MLR model (blue) and extracted by SSA (red) Right axis: the EESC curve (cyan). The vertical dotted line (purple) indicates the location of the maximum of EESC in February 1997. The minimum of the nonlinear SSA is between August 1996 and January 1997.*

Conference material:

- Fragkos, K., Taylor, M., Bais, A., Fountoulakis, I., Tourpali, K., Meleti, C., Zempila, M.M. (2016) *Multi-decadal trend analysis of total columnar ozone over Thessaloniki*. In: Perspectives on Atmospheric Sciences, Springer Atmospheric Sciences, ISBN: 978-3-319-35094-3, Proceedings

## 2.7 Spatiotemporal 3D analysis of oscillations in global ozone

In the last few decades, ozone research has been strongly shaped by the observation that anthropogenic chlorofluorocarbons can deplete the ozone layer, the discovery of the ozone hole, and the signing and impact of the Montreal Protocol to limit the production and concentration of ozone-depleting substances. As we move towards ozone recovery, the focus of attention is shifting towards analysis of long-term ozone changes associated with declining halogen loads, polar ozone depletion and increases in greenhouse gases, and short-term ozone changes related to internal variability like the QBO, ENSO and NAO, or to external forcings such as volcanic signals, or the 27-day and 11-year cycles in solar variability. For all of these, accurate knowledge of the zonal latitude, altitude and seasonal/temporal structure of the ozone response is required to place constraints on possible explanations (in other words a 2D+1 spatiotemporal modeling framework). In this study we use the SBUV "Merged Cohesive" dataset of satellite ozone observations provided by the WCRP/SPARC-SI2N framework (SPARC, IO3C, IGACO-O3 and NDACC) which spans the latitudinal zonal range: 80N–80S in 5 degree intervals, the altitude from 50–0.5 hPa in 13 Dobson layers, and the period 11/1978 – 12/2013 with daily and monthly-averages. The dataset is of high quality, stable (trends in TOC vary by only about 1%/decade) and multi-decadal; making it suitable for the study of long-term effects. It also has the required spatial and temporal coverage for a study of short-term effects and external forcings. In this study we apply the continuous wavelet transform to each of the time series in the 2D spatial grid (latitudinal zones x Dobson layers) spanning the global domain to calculate the wavelet power spectrum and to identify statistically-significant periods for each time series. We then construct 3D grids of constant period contours in the 2+1D space to trace and study the spatiotemporal variation of individual oscillations. In parallel, we also apply singular spectrum analysis to each time series to extract non-prescribed/nonlinear trends and construct a 3D grid for studying the global long-term behaviour, transitions and temporal change-points in the data. Finally, we investigate causal interactions between oscillatory modes in the 2+1D space using advanced causal discovery algorithms in an attempt to connect them with the underlying dynamics.

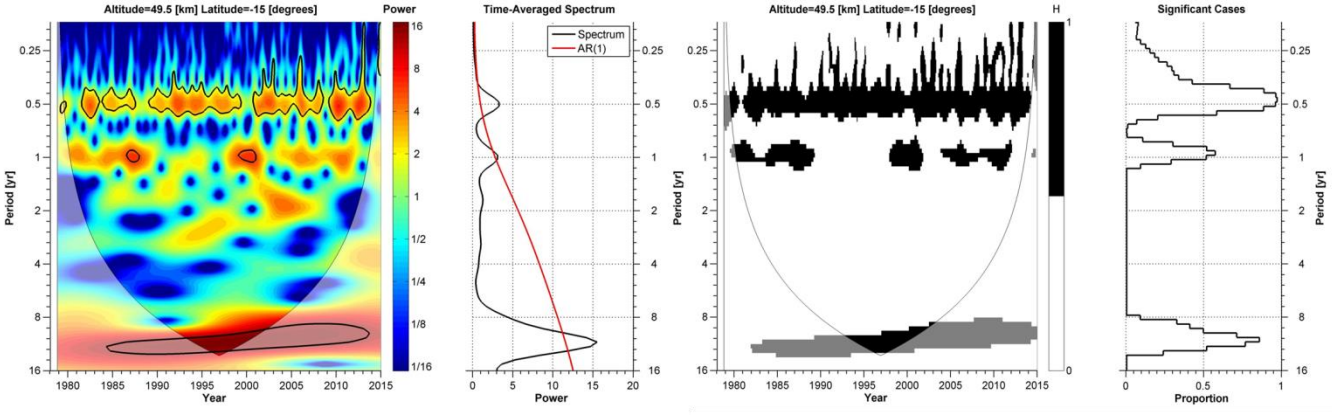

***Figure 7a.*** *(left) The wavelet power spctrum of the ozone layr time series at 49.5km and 15oS together with the time-averaged spectrum and the AR(1) reference curve. (right) Months where oscillations are statistically-significant at the 95% level and their prevalence as a proportion of the time series of 434 monthly values.*

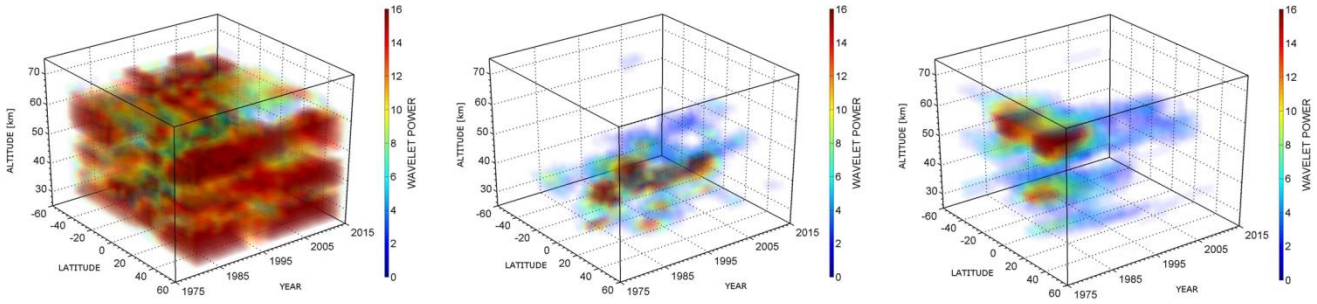


***Figure 7b.*** *2D+1 distribution of wavelet power for 3 key oscillations: (left) the annual cycle ≈ 12 months (1.0 yr), (center) the Quasi-Biennial Oscillation ≈ 28 months (2.3 yr) (right) modulation by volcanic activity of the Solar flux ≈ 84 months (7.0 yr).*

Conference material:

- Taylor, M., Fragkos, K., Koukouli, M.E., Tourpali, K., Misios, S., Bais, A., Balis, D.S., Ghil, M., Harris, N.R.P., Hassler, B., Runge, J., Tummon, F., Wild, J., Zempila, M.M. (2016) *A global description of oscillations and trends in multi-decadal ozone from spectral analysis of zonally-averaged merged satellite data*. **Quadrennial Ozone Symposium (QOS) 2016, 4–9 September 2016 Edinburgh**. http://www.ozone-symposium-2016.org. [Poster]

## 2.8 Nowcast of surface solar radiation as a function of TOC and cloud

In support of the Horizon 2020 project Geo-Cradle (http://www.geocradle.eu/index.php/about-geocradle/work-packages) and the solar energy application (SOLEA) team (www.solea.gr) I have developed a neural network (NN) model of the direct normal irradiance (DNI) and global horizontal irradiance (GHI) **gridded spectrum** as a function of satellite cloud type (ice of water cloud), cloud optical depth (COT), TOC the solar zenith angle (SZA) and aerosol parameters: aerosol optical depth (AOD), single scattering albedo (SSA), columnar water vapour (H2O) and the Angstrom Exponent (AEX). The cloud inputs (cloud type and COT) are taken from MSG-2 and the AOD is provided by the CAMS model forecast. The SZA is computed for every pixel of the satellite domain. Climatological values are used for the other parameters. The output is an estimated nowcast map where each pixel contains the DNI or the GHI spectrum. The spectral integration of provides maps of the total DNI or GHI in each pixel at each nowcast timestamp (every 15 mins for MSG-2 data). I have coded the calculation and mapping chain in MATLAB. Precision can be increased when aerosol data is also provided by geostationary satellite.

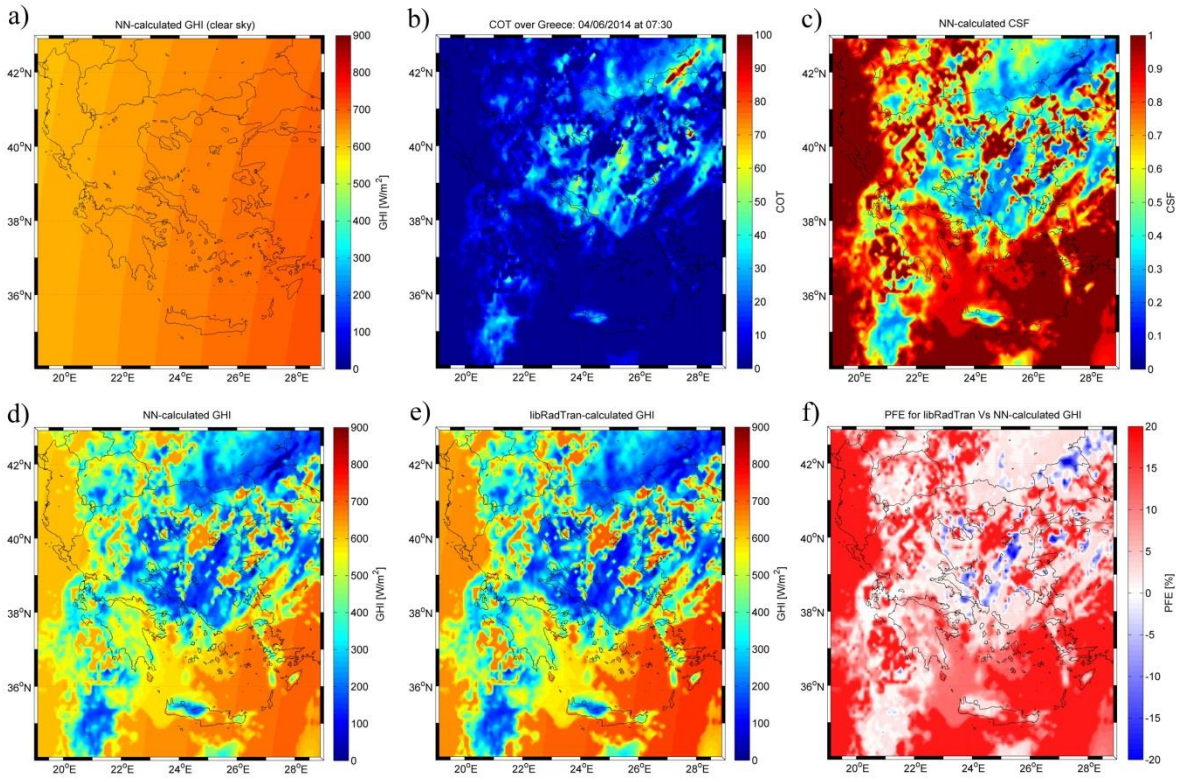


***Figure 8.*** *The spectrally-integrated 'clear sky' GHI map for the ROI (54,531 pixels) at 07:30am UGT. Note that, at this time of the morning in Greece, the sun is situated nearly due East. b) The COT map obtained from MSG3 satellite measurements of ICOT and WCOT by the SEVIRI instrument and associated cloud products. c) The CSF map. d) The spectrally-integrated GHI map generated by the cloudy sky NN. e) The spectrally-integrated GHI map generated by libRadtran for the same inputs. f) The PFE resulting from the difference between the spectrally-integrated GHI map generated by libRadtran and the cloudy sky NN.*

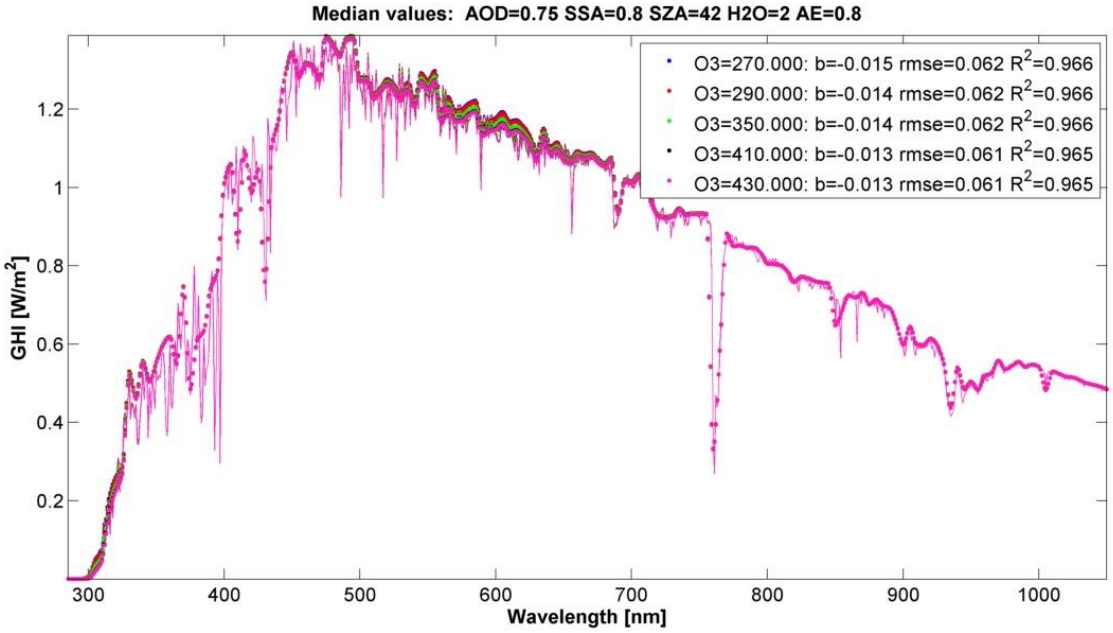


***Figure 9.*** *The libRadtran GHI spectrum (lines) overlaid with NN estimated (dots) for the case of high aerosol load. The 5 colour codes correspond to the comparison of the NN output and libRadtran for differing levels of TOC.*

Scientific articles published and conference materials:

- Taylor M, Kosmopoulos PG, Kazadzis S, Keramitsoglou I, Kiranoudis CT (2016) *Neural network radiative transfer solvers for the generation of high resolution solar irradiance spectra parameterized by cloud and aerosol parmeters.* **Journal of Quantitative Spectroscopy and Radiative Transfer** 168: 176-192. www.dx.doi.org/10.1016/j.jqsrt.2015.08.018.
- Kosmopoulos PG, Kazadzis S, Taylor M, El-Askary HM, Raptis PI, Keramistsoglou I, Kiranoudis C (2016) *Estimation of the solar energy potential in Egypt by developing high resolution solar Atlas and nowcasting service in real time*. **American Geophysical Union (AGU) Fall Meeting 2016, 12-16 December, San Francisco, USA.** https://fallmeeting.agu.org/2016/. [abstract submitted]
- Kosmopoulos, P.G., Kazadzis, S., Taylor, M., Bais, A., Lagouvardos, K., Kotroni, V., Keramitsoglou, I., Kiranoudis, C. (2016) *Estimation of the solar energy potential in Greece using satellite and ground-based observations*. In: Perspectives on Atmospheric Sciences, Springer Atmospheric Sciences, ISBN: 978-3-319-35094-3, Proceedings of the **13th International Conference on Meteorology, Climatology and Atmospheric Physics (COMECAP) 2016, 16-19 September, Thessaloniki, Greece**. http://comecap2016.geo.auth.gr. [Paper + Talk]
- Kosmopoulos P, Taylor M, Kazadzis S (2016). *A model of dust episode impact on surface solar irradiance*. **International Skynet Workshop (ISW), 2-4 March, Rome, Italy**. http://romaskynet.artov.isac.cnr.it/images/Monica/Program.pdf. [Talk]

## 2.9 Data Products Produced

A summary of the ozone, SO2, Ozone and UV radiance datasets produced in this work is collected in the table below:

| Product | Abbreviation | Parameter |
|---|---|---|
| 1 | TOC | Total ozone column linear trend [DU/decade] & nonlinear (SSA) trend |
| 2 | SBO | SBUV layer ozone trend in each Dobson layer + zonal averaged latitude |
| 3 | SO2 | Linear trend [DU/decade] for a sample of 150 Chinese cities & power statons |
| 4 | PAR | Photosynthetically-Active Radiation [W/m2] |
| 5 | GHI | Global Horizontal Irradiance [W/m2] |
| 6 | CIE | Erythemal UV irradiance from NILU-NN |

| | | |
|---|---|---|
| 7 | VID | Vitamin D effective dose from NILU-NN |
| 8 | DNA | DNA damage dose from NILU-NN |
| 9 | SSR | (gridded) surface solar radiation (DNI & GHI) spectra from NN solver |

### 2.10 CHIMERE chemical transport model

I dowloaded and helped support the installation of Version 2014b of the CHIMERE model (http://www.lmd.polytechnique.fr/chimere) at AUTh/grid under Unix. Considerable editing of configuration scripts for running the MPI parallel processing interface/module(s) was needed even to run the demo script. This was finally achieved with the support of Alexandra Georgi and Serafeim Kontos. The test run spans continental Europe ("CONT5" domain), has resolution: horizontal = 45km, vertical = 30 levels, and the 8-day period: March 12-19, 2009. Meteorological Forcing is provided by a WRF simulation driven by the 6-hourly NCEP/AVN analyses with the spectral "nudging" option (grid FDDA). The characteristic of this run is that a strong PM pollution event. The upper-left plot is the output from the CHIMERE test run fed to the CHIMPLOT post-processing package in Python. The upper-right visualization is the 4D visualization of the PM10 field I wrote in MATLAB. The other panels show other important components of air quality ($NOx$,$SO_2$,$CO$,$O_3$).

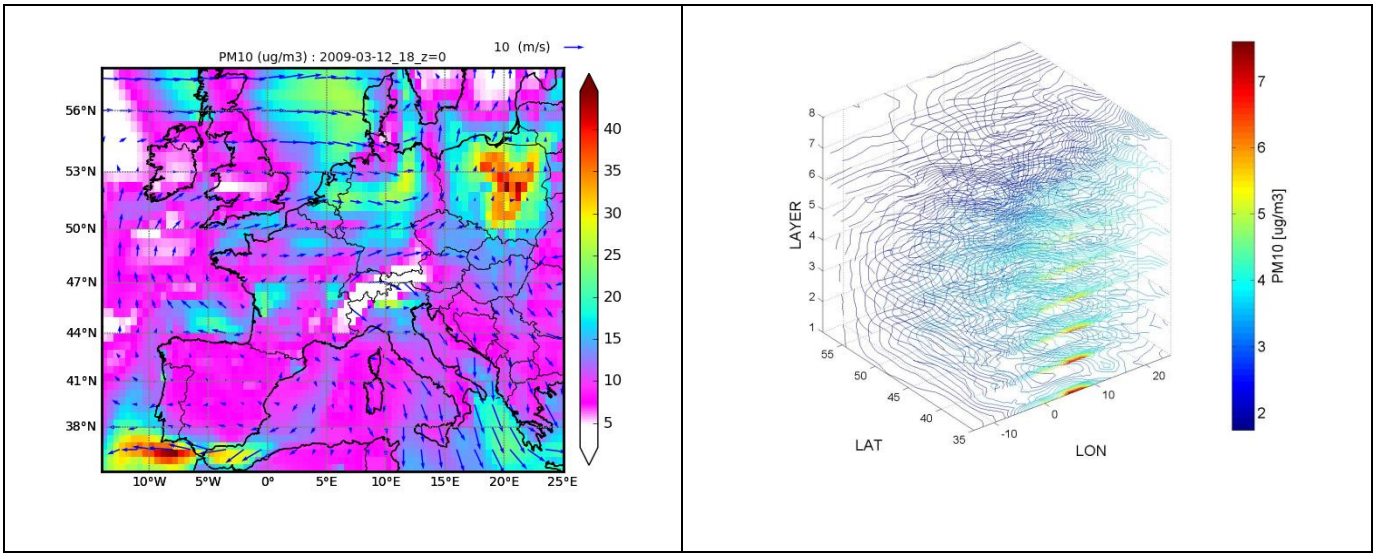

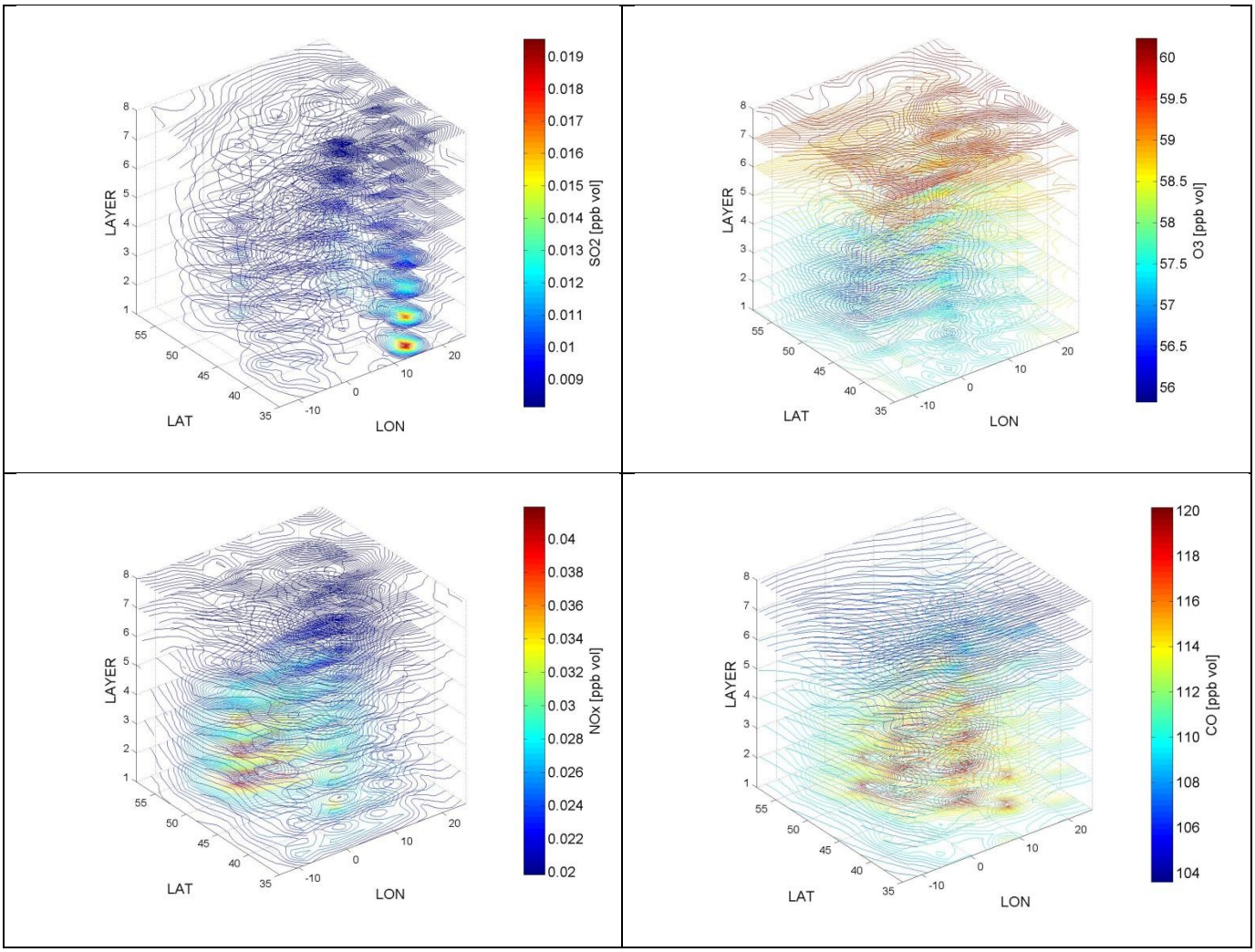


We are currently working on setting up a nested run for Europe with increased density over Greece and the Balkans and with the highest resolution sub-domains centered over Thessaloniki and Athens. In this, I provided input to the set up of WRF layering by calculating the density of vertical layers for various parameterizations:

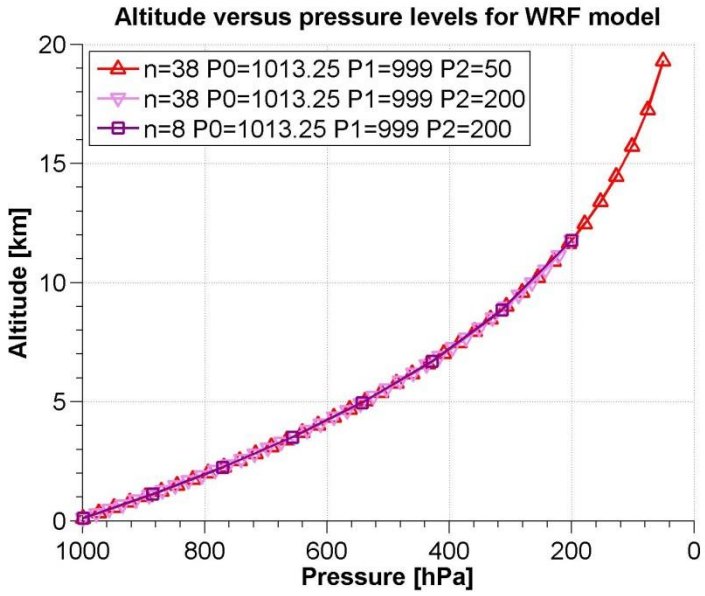


The final domain choice was determined to a large extent by the availability of chemical concentration fields and Christos Giannaros is preparing e WRF run for these parameters. Below is the full modeling domain set-up:

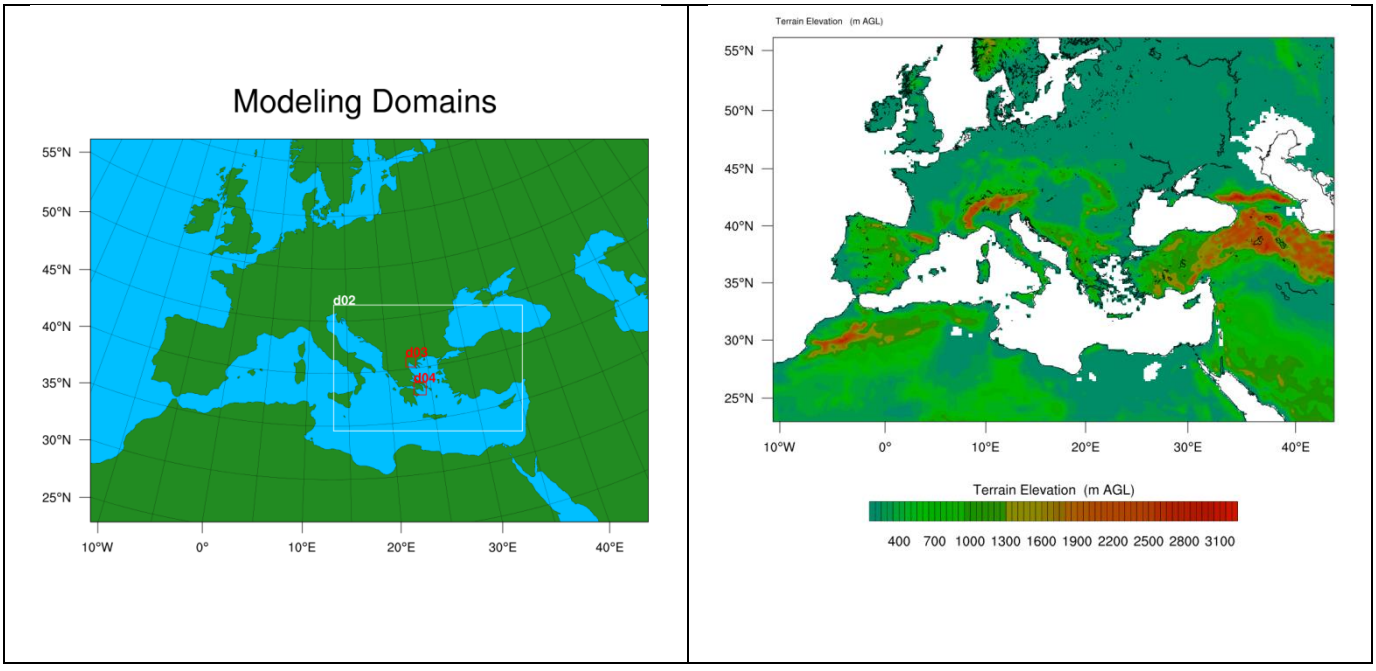

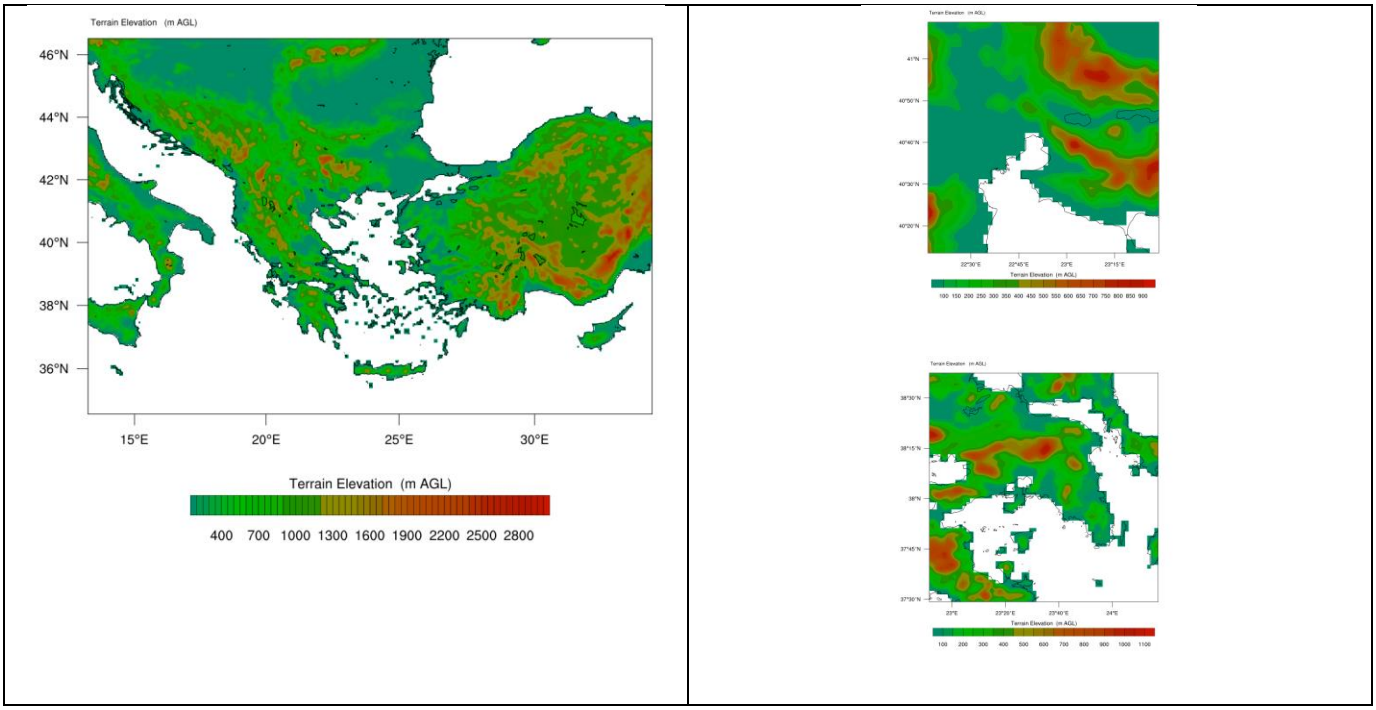


I hope to be able to continue this work from October and help support the team implementing a full run complete with emission fields. With 4D model output concentration fields, I will be able to help in data analyses (e.g. comparison with LIDAR profiles and satellite columns etc) and to help support the development of a 3D model of air quality.

## 3. SUMMARY

This research has produced a number of novel atmospheric physics algorithms and models for the study of climate:

- the creation of a long timeseries of TOC from NILU-UV irradiances
- the creation of long timeseries of biological UV products from NILU-UV irradiances inclouding: CIE, Vitamin D, DNA damage and plant growth
- the capacity to derive photosynthetically-active radiation (PAR) from total global horizontal irradiance (GHI) timeseries and vice-versa across a network of UV monitoring stations *with a single model*
- a new high frequency (1-minute) cloud filter based on SSA applied to NILU-UV irradiances in the UV and the visible
- a new automated time series decomposition code (produced as part of the China SO2 study) that automates the process of gap-filling and which also isolates noise
- a new automated detector of statistically-significant periods in time series of trace gases like TOC and SO2
- a new wavelet-based 3D analysis of the spatio-temporal distribution of global ozone in SBUV monthly averaged values in various Dobson layers than are also zonally-averaged in latitude.

In addition, technical input was provided to assist in the installation, set-up and test-running of the CHIMERE chemical transport model at AUTh-grid. Post-processing visualization scripts were also written. In parallel, neural network models of surface solar radiation with ozone as an explicit input variable have been developed together with associated map visualization code in MATLAB. Transfer of knowledge to

LAP-AUTh of these skills can provide the capability for nowcasting the new products developed here. It is hoped that these will help provide the capacity for participation in new and ongoing EO studies of climate and will help further enhance the substantial scientific effort being made by colleagues at LAP-AUTh.

## ACKNOWLEDGEMENTS

I am grateful to Prof. Dimitris Balis for hosting me at LAP-AUTh and to Mariliza Koukouli, Melina Zempila, Ilias Fountoulakis and Kostas Fragkos for kindly making available ground-based measurements and satellite datasets and for their useful input during algorithm and model devlopement. I am also grateful to Alexandra Georgi at AUTh-grid and Makis Kontos for UNIX technical support during the installation and testing of CHIMERE, and to Eirini Zyrichidou and Natasa Poupkou for helping establish the parameters of the initial run and to Christos Giannaros for preparing WRF runs. The research was carried out in the framework of the project "*Construction of ozone datasets for the study of climate*" under the supervision of the research dirctor Professor D.S. Balis from 2/3/2016 to 30/9/2016 (C/N 91224) funded by ESA-Phase II/Belgian Institute for Aeronomy (BIRA-IASB).